DMD Fast Forward. Published on July 19, 2019 as DOI: 10.1124/dmd.119.087973
This article has not been copyedited and formatted. The final version may differ from this version.

DMD # 87973

Prediction of tissue - plasma partition coefficients using microsomal partitioning: Incorporation into physiologically-based pharmacokinetic models and steady state volume of distribution predictions

Kimberly Holt, Min Ye, Swati Nagar, and Ken Korzekwa

Department of Pharmaceutical Sciences, Temple University School of Pharmacy, 3307 N Broad Street, Philadelphia, Pennsylvania 19140

DMD Fast Forward. Published on July 19, 2019 as DOI: 10.1124/dmd.119.087973
This article has not been copyedited and formatted. The final version may differ from this version.

DMD # 87973

Running Title: Prediction of tissue - plasma partition coefficients

Corresponding Author: Ken Korzekwa, 3307 N Broad St. Philadelphia, PA 19140,

215-707-7892, korzekwa@temple.edu

# of words in the Abstract: 230

# of words in the Introduction: 749

# of words in the Discussion:1495

List of non-standard abbreviations used in the paper: absolute average fold error (AAFE), acidic phospholipid (AP), area under curve (AUC), blood to plasma ratio (BP), clearance (Cl), concentration in plasma (Cp), concentration-time (c-t), unbound concentration in plasma (C_{up}), vegetable oil: water partition coefficient (Pvo), exposure overlap coefficient (EOC), fractional acidic phospholipids (f_{apl}), fraction extracellular water (f_{ew}), fraction intracellular water (f_{iw}), fraction neutral lipids (f_{nl}), fraction unbound in microsomes (f_{um}), fraction unbound in plasma (f_{up}), fraction of neutral lipids (f_{nl}), fraction of neutral phospholipids (f_{npl}), tissue: plasma partition coefficient (Kp), unbound tissue: plasma water partition coefficient (Kp_u), differential phospholipid K_p prediction method ($K_{p,dPL}$), membrane-based K_p prediction method ($K_{p,mem}$), liquid chromatography (LC), log of the octanol: water partition coefficient (LogP), mass spectrometry (MS), non-compartmental analysis (NCA), neutral lipid (NL), neutral phospholipid (NP), octanol: water partition coefficient (P), physiologically-based pharmacokinetic (PBPK), pharmacokinetics (PK), pKa,a (ionization constant for acids), pKa,b (ionization constant for bases), plasma protein binding (PPB), rat liver microsomes (RLM), steady-state volume of distribution (V_{ss})

DMD Fast Forward. Published on July 19, 2019 as DOI: 10.1124/dmd.119.087973
This article has not been copyedited and formatted. The final version may differ from this version.

Abstract

Drug distribution is a necessary component of models to predict human pharmacokinetics. A new method ($K_{p,mem}$) to predict unbound tissue to plasma partition coefficients (K_{pu}) was developed using in vitro membrane partitioning (f_{um}), plasma protein binding (f_{up}), and LogP. The resulting K_p values were used in a physiologically based pharmacokinetic (PBPK) model to predict the steady-state volume of distribution (V_{ss}) and concentration-time (C-t) profiles for 19 drugs. These results were compared with Kp predictions using a standard method ($K_{p,dPL}$) that differentiates between acidic and neutral phospholipids. The $K_{p,mem}$ method was parameterized using published rat K_{pu} data and tissue lipid composition. The K_{pu} values were well predicted with R^2 = 0.8. When used in a PBPK model, Vss predictions were within 2-fold error for 12 of 19 drugs with $K_{p,mem}$ versus 11 of 19 for $K_{p,dPL}$. With one outlier removed for $K_{p,mem}$ and two for $K_{p,dPL}$, the V_{ss} prediction R^2 was 0.80 and 0.79 for the $K_{p,mem}$ and $K_{p,dPL}$ methods respectively. C-t profiles were also predicted and compared. Overall, the $K_{p,mem}$ method predicted Vss and C-t profiles equally or better than the $K_{p,dPL}$ method. An advantage of using f_{um} to parameterize membrane partitioning is that f_{um} data is used for clearance prediction and is therefore generated early in the discovery/development process. Also, the method provides a mechanistically sound basis for membrane partitioning and permeability for further improving physiologic PK models.

Significance Statement

A new method to predict tissue-plasma partition coefficients was developed. The method provides a more mechanistic basis to model membrane partitioning.

Keywords

Tissue : plasma partition coefficients, volume of distribution, membrane partitioning, PBPK modeling

DMD Fast Forward. Published on July 19, 2019 as DOI: 10.1124/dmd.119.087973
This article has not been copyedited and formatted. The final version may differ from this version.

Introduction

Volume of distribution and clearance equally determine the half-life of a drug. V_{ss} can be predicted using empirical methods (Obach et al., 1997), computational approaches (Ghafourian et al., 2004; Lombardo et al., 2006; Zhivkova and Doytchinova, 2012), physiologic equations (Oie and Tozer, 1979; Lombardo et al., 2004; Korzekwa and Nagar, 2017a), and with tissue: plasma partition coefficients (K_p). K_p prediction methods are widely used since they describe distribution in PBPK models. While some methods require an in vivo component (Arundel, 1997; Björkman, 2002; Jansson et al., 2008; Poulin and Theil, 2009), others use more readily available in vitro inputs.

Several factors influence drug distribution, including partitioning into membranes and other lipids, binding to proteins (primarily plasma proteins), pH partitioning (e.g. lysosomes), transporters, and membrane permeability. Most models represent tissue interactions with in vitro surrogates. The Poulin and Krishnan model originally described phospholipid partitioning with the octanol: water partition coefficient (P) and assumed phospholipid composition to be represented by 30% octanol and 70% water (Poulin and Krishnan, 1995). They developed K_p prediction equations, which included an additional surrogate for neutral lipid partitioning in adipose tissue (Poulin and Theil, 2000; Poulin et al., 2001), which was modified by Berezhkovskiy (Berezhkovskiy, 2004). Rodgers and Rowland developed two equations for prediction of unbound K_p (K_{pu}): one for acids, neutrals, and weak bases, and another for moderate to strong bases (Rodgers et al., 2005; Rodgers and Rowland, 2006). Drug partitioning into erythrocytes was used to parameterize the interaction of bases with acidic phospholipids. It was assumed that ionized bases interact only with acidic phospholipids, while uncharged molecules interact only with neutral phospholipids (Rodgers et al., 2005; Rodgers and Rowland, 2006).

In most currently used composition-based models, LogP is used to model the phospholipid partitioning (0.3 P). A shortcoming of using LogP to represent phospholipid partitioning is the lack of orientation-specific interactions with phospholipid membranes (Balaz, 2009; Nagar and Korzekwa, 2012; Nagar and Korzekwa, 2017). Additionally, both neutral and ionized bases are known to interact with all phospholipids, and not just net-neutral and net-acidic phospholipids, respectively. Therefore, current methods to calculate K_p appear to be based on mechanistically unsound assumptions. Previously, we used microsomal partitioning (f_{um}) instead of LogP to parameterize phospholipid

DMD Fast Forward. Published on July 19, 2019 as DOI: 10.1124/dmd.119.087973
This article has not been copyedited and formatted. The final version may differ from this version.

partitioning in V_{ss} model (Korzekwa and Nagar, 2017a). Partitioning into microsomes (unsorted phospholipid vesicles) is used extensively in clearance predictions, can be determined experimentally, or can be predicted (Austin et al., 2002; Hallifax and Houston, 2006; Poulin and Haddad, 2011; Nagar and Korzekwa, 2017). A benefit of using f_{um} to represent phospholipid partitioning is that it measures interactions with all phospholipids for both charged and uncharged species.

Previous studies have compared different K_p prediction methods and their ability to predict both tissue K_p and/or V_{ss} (De Buck et al., 2007; Poulin and Theil, 2009; Jones et al., 2011; Graham et al., 2012; Zou et al., 2012; Chan et al., 2018). These studies came to different conclusions on the most accurate K_p model, primarily dependent on the drug dataset used (De Buck et al., 2007; Graham et al., 2012). Graham et al. showed that the Rodgers et al. method was able to better predict K_p and V_{ss} for different classes of drugs than other composition-based models. The Poulin and Theil method led to good V_{ss} predictions, but required in vivo data (K_{pu} muscle)(Poulin and Theil, 2009; Graham et al., 2012). More recently, Chan et al. compared the ability of composition-based K_p models and preclinical extrapolation to predict V_{ss}. Composition-based models predicted V_{ss} with accuracy similar to preclinical extrapolation. They noted that the Rodgers method was able to predict V_{ss} well for drugs with LogP values less than 3, and that many drugs with large errors in V_{ss} for composition-based models, also had errors in preclinical extrapolation (Chan et al., 2018).

This report evaluates a model to predict K_p using f_{um} to represent membrane partitioning. Plasma protein binding and microsomal partitioning were determined experimentally for nineteen drugs. Tissue K_p values were calculated for each compound using a differential phospholipids method ($K_{p,dPL}$ (Rodgers et al., 2005; Rodgers and Rowland, 2006)), as well as a method that uses f_{um} to parameterize membrane partitioning ($K_{p,mem}$). Simulations were run and their ability to predict V_{ss} and concentration-time profiles determined. More mechanistically sound assumptions for K_{pu} will be required when expanding current perfusion-limited PBPK models to include explicit membrane partitioning and permeability. Models to predict K_{pu} bases on experimental partitioning into membranes may allow a facile transition to models that limit permeability with explicit membrane compartments (Nagar et al., 2014).

Materials and Methods

Materials

A Harvard Apparatus 96-well equilibrium dialyzer and single-plate Harvard Apparatus (Holliston, MA) plate rotator were used for equilibrium dialysis experiments. Human plasma was obtained from U.S. Biological (Salem, MA) and Innovative Research Inc (Novi, MI). Rat liver microsomes (RLM) were obtained from BD Biosciences (San Jose, CA) and Corning Life Sciences (Tewksbury, MA). Warfarin, fluconazole, glyburide (glybenclamide), ketoprofen, fenofibrate, +/cis diltiazem hydrochloride, +/- verapamil hydrochloride, caffeine, betaxolol hydrochloride, dimethyl sulfoxide (DMSO), nicardipine hydrochloride, metoprolol tartrate, felodipine, and nafcillin sodium were obtained from Sigma Aldrich (St. Louis, MO). Quinidine gluconate, formic acid, acetonitrile, and diphenhydramine hydrochloride were obtained from Fisher Scientific (Norristown, PA). Mibefradil hydrochloride was obtained from Cayman Chemical Company (Ann Arbor, MI). Diclofenac sodium was obtained from Calbiochem (Burlington, MA). Fenofibric acid was obtained from Kano Laboratories (Nashville, TN). One mg/mL solutions of phenytoin, diazepam, and midazolam in methanol were obtained from Cerilliant (a Sigma Aldrich company). The 100 mM PBS and 0.3 mM $MgCl_2$ dialysis buffer was composed of magnesium hydrochloride hexahydrate (Fisher Scientific), potassium phosphate monobasic (Sigma), and potassium phosphate dibasic (Fisher Scientific). An Agilent 1100 HPLC and API 4000 mass spectrometer and Agilent 1100 HPLC and API 4000 Q-Trip mass spectrometer were used to determine the concentrations for equilibrium dialysis. Mathematica v 11.0. (Wolfram, Champaign, IL) was used for all compartmental modeling and simulations. Literature data from plots were digitized using Engauge Plot Digitizer v 10.4.

Probe Drug Selection and Data Collection

A diverse set of drugs, made up of acids, bases, and neutrals, was selected to compare prediction methods (Table 1). Drugs were considered neutral when primarily uncharged at physiological pH (7.4). Unless noted otherwise, the acidic and basic pK_a values ($pK_{a,a}$ and $pK_{a,b}$) for neutrals was set at 14 and 1 respectively. Any significant ionized and neutral fraction is considered by both methods. The probe drugs were selected based on the availability of literature IV PK data, as well as drug specific parameters. Average experimental IV bolus and/or infusion C-t profiles for 19 drug studies were

collected from the literature. If the data was represented as graphical concentration-time profiles, the plots were digitized. When average subject weight was available, simulations were conducted to reproduce the observed Vss for that average weight. The observed clearance and the steady-state volume of distribution were determined by compartmental analysis using standard equations with Mathematica. Specifically, one- to three-compartment models were evaluated to generate the C-t profiles from the experimental data. Experimental clearance and V_{ss} values were determined from these compartmental models. The best model for the experimental data was determined by AICc values (Akaike, 1974) and residual plots. For all drugs, microrate constants were well defined and use of non-compartmental analysis was not required. Experimental clearance values were assumed for all further modeling efforts and experimental V_{ss} values were compared to predicted values.

Literature physiological data were used for K_p predictions and PBPK modeling (Brown et al., 1997; Poulin and Theil, 2002; Fenneteau et al., 2010; Ye et al., 2016). For drug specific parameters (LogP, pK_a, and BP, Table 2), experimental values from the literature were preferred over calculated/predicted values, and if more than one experimental value was found, then the experimental values were averaged. Human BP values could not be found for betaxolol and nafcillin. For betaxolol, the f_{up} values are similar for rat and human, and therefore the rat BP value of 2.0 was used. For nafcillin, a value of 0.55 (1-hematocrit) was used, which is the BP ratio of similar compounds in humans (Greene et al., 1978). Also, this will not affect V_{ss} predictions since BP is not included in the K_p equations for acids. Protein binding was experimentally determined for all compounds (Table 2), with the exception of caffeine due to caffeine contamination in all plasma samples. A caffeine f_{up} value of 0.72 was determined by averaging values found in the literature.

The $LogP_{vo}$ (log of the vegetable oil: buffer partition coefficient) was calculated from LogP using equation 1 (Leo et al., 1971). This term is used to represent neutral lipid partitioning in adipose tissue in the $K_{p,dPL}$ method; however, it is not used in the $K_{p,mem}$ prediction method.

$$LogP_{vo} = 1.115 \cdot LogP - 1.35 \qquad \text{Eq. 1}$$

Microsomal Partitioning and Plasma Protein Binding

DMD Fast Forward. Published on July 19, 2019 as DOI: 10.1124/dmd.119.087973
This article has not been copyedited and formatted. The final version may differ from this version.

Equilibrium dialysis was used to determine the fraction unbound in plasma (f_{up}) and microsomes (f_{um}) for the probe drugs using a protocol modified from prior studies (Kochansky et al., 2008; Curran et al., 2011; Di et al., 2017). Human plasma was adjusted to pH 7.4 by adding 1 M HCl. For f_{um} determination, a 0.5 mg/mL rat liver microsomal solution was prepared from a 20 mg/mL pooled rat liver microsome stock solution. For highly bound compounds, a dilution method was used. Plasma was diluted using a 100 mM phosphate buffer and 3 mM $MgCl_2$ solution to either 50% or 10% plasma. A 50% dilution of plasma was used for warfarin, while a 10% dilution was used for ketoprofen, nicardipine, glyburide, diclofenac, felodipine, and mibefradil. Drug solutions (2 μM) in either plasma or microsomes were added to wells on one side of the dialyzer, and blank 100 mM phosphate buffer with 3 mM of $MgCl_2$ was added to the other side. The dialyzer plate was placed in the plate rotator, set to a speed of approximately 22 rotations per minute, and incubated for 22 hours at 37 degrees Celsius and 5% CO_2. LC-MS/MS was used for the determination of the concentration of drug in the buffer and the matrix.

The fraction unbound in a given matrix was determined by dividing the concentration of drug on the buffer side by the concentration of drug on the matrix side. For protein binding experiments using the dilution method, the f_{up} is calculated by Equation 2:

$$f_{up} = \frac{1/D}{\left(\left(\frac{1}{f_{u,d}}\right)-1\right)+1/D} \qquad \text{Eq. 2}$$

Where D is the dilution factor, $f_{u,d}$ is the fraction unbound in plasma measured in the diluted matrix, and f_{up} is the fraction unbound in plasma.

Experimental f_{um} values were measured at microsomal concentrations between 0.5 mg/mL and 2 mg/mL, and converted to values for 1 mg/mL (Equation 3) (Austin et al., 2002):

$$f_{u2} = \frac{1}{\frac{C_2}{C_1}\left(\frac{1-f_{u1}}{f_{u1}}\right)+1} \qquad \text{Eq. 3}$$

where f_{u2} is the corrected unbound fraction, C_2 is the 1 mg/mL microsomal protein concentration, C_1 is the microsomal protein concentration used in assay, and f_{u1} is the fraction unbound in matrix measured during the assay.

DMD Fast Forward. Published on July 19, 2019 as DOI: 10.1124/dmd.119.087973
This article has not been copyedited and formatted. The final version may differ from this version.

The average fraction unbound, standard deviation (SD), and the coefficient of variation (CV) were determined for each assay.

Simulations

A generic PBPK model was used, with different tissues represented by 10 compartments (adipose, bone, brain, gut, kidney, liver, lungs, muscle, skin, spleen), representing the major tissues in the body, Figure 1. These compartments are linked via arterial and venous blood flows. K_p values were predicted for each of the tissues using both methods ($K_{p,dPL}$ and $K_{p,mem}$). The original $K_{p,dPL}$ method uses two separate equations, one for acids, weak bases, and neutrals, and another for moderate-to-strong bases (Equations 4 -7)(Rodgers et al., 2005; Rodgers and Rowland, 2006).

The $K_{p,dPL}$ equation used for prediction of Kpu for strong-to-moderate bases :

$$K_{pu,tissue} = f_{ew} + \frac{1+10^{pKab-pHiw}}{1+10^{pKab-pHp}} \cdot f_{iw} + \frac{K_{AP}\cdot[AP]\cdot 10^{pKab-pHiw}}{1+10^{pKab-pHiw}} + P \cdot f_{nl} + \frac{(0.3P+0.7)\cdot f_{npl}}{1+10^{pKab-pHp}} \quad \text{Eq .4}$$

where few is the fractional volume of extracellular water, f_{iw} is the fractional volume of intracellular water, P is the octanol: water partition coefficient, [AP] is the concentration of acidic phospholipids in the tissue, Kap is the association constant for acidic phospholipids in the tissue, f_{nl} is the fractional volume of neutral lipids, f_{npl} is the fractional volume of neutral phospholipids, pKab is the basic ionization constant, pKaa is the acidic ionization constant.

The Rodgers equation used for prediction of Kpu for acids, neutrals, and weak bases:

$$K_{pu,tissue} = f_{ew} + \frac{1+10^{pHiw-pKaa}}{1+10^{pHp-pKaa}} \cdot f_{iw} + \frac{P\cdot f_{nl}+(0.3P+0.7)\cdot f_{NP}}{1+10^{pHp-pKaa}} + \left(\frac{1}{f_{up}} - 1 - \left(\frac{P\cdot f_{nl}+(0.3P+0.7)\cdot f_{NP}}{1+10^{pHp-pKaa}}\right)\right) \cdot \frac{[PR]_T}{[PR]_P}$$

Eq .5

where $[PR]_T/[PR]_P$ is the plasma protein tissue (extracellular fluid) to plasma ratio.

For Eq. 4, the association constant for blood cells is defined in equation 6, and the tissue: plasma water partitioning coefficient for the blood cells is defined in equation 7.

DMD Fast Forward. Published on July 19, 2019 as DOI: 10.1124/dmd.119.087973
This article has not been copyedited and formatted. The final version may differ from this version.

$$K_{a,BC} = (Kp_{u,BC} - \frac{1+10^{pka-pHBC}}{1+10^{pKa-pHp}} F_{iw,BC} - \frac{P_{ow} \cdot f_{nl,BC} + (0.3P_{ow}+0.7) f_{np,BC}}{1+10^{pka-pHp}}) \cdot (\frac{1+10^{pKa-pHp}}{[AP^-]_{BC} 10^{pKa-pHBC}})$$ Eq. 6

$$Kp_{u,BC} = \frac{BP+H-1}{H \cdot f_{up}}$$ Eq. 7

The tissue: plasma partition coefficient (K_p) can be determined from K_{pu} by equation 8:

$$Kp = Kp_u \cdot f_{up}$$ Eq. 8

For the $K_{p,mem}$ method we use the previously reported equation (Korzekwa and Nagar, 2017a) that considers both phospholipid membrane partitioning with f_{um} and neutral lipid partitioning with P (Equation 9):

$$Kp_{tissue} = r(1 - f_{up}) + f_{iw} \cdot f_{up} \cdot \frac{10^{pKab-7.0}+10^{7.0-pKaa}+1}{10^{pKab-7.4}+10^{7.4-pKaa}+1} + f_{ew} \cdot f_{up} + f_{pl} \cdot \frac{10^{pKab-7.0}+10^{7.0-pKaa}+1}{10^{pKab-7.4}+10^{7.4-pKaa}+1} \cdot f_{up} \cdot a \cdot LKL + \frac{f_{nl} \cdot f_{up} \cdot b \cdot P}{10^{pKab-7.0}+10^{7.0-pKaa}+1}$$ Eq. 9

where r is the protein ratio between the tissue and plasma, f_{pl} is fractional volume of phospholipid, LKL is the lipid binding constant, P is the octanol water partition coefficient, and a and b are parameterized coefficients. Plasma and tissue pH values were assumed to be 7.4 and 7.0, respectively. As described previously for V_{ss} predictions (Korzekwa and Nagar, 2017a), the tissue-specific r values for bases were decreased by 2.23 fold due to the lower amount of α-acid glycoprotein in the extracellular fluid relative to albumin (Rowland and Tozer, 2011).

Neutral lipid partitioning in adipose tissue is described by the vegetable oil: water partition coefficient in the $K_{p,dPL}$ method, which is generally calculated from LogP. In the $K_{p,mem}$ prediction method LogP is used directly. The a and b terms in Eq. 9 were parameterized using the tissue K_p values and tissue composition data from Rodgers (Rodgers et al., 2005; Rodgers and Rowland, 2006). We excluded zwitterions and combined neutral and acidic phospholipids to obtain a fraction total phospholipids. Most f_{um} values were calculated with our previously reported model (Nagar and Korzekwa, 2017) since experimental values are not available for this dataset. Log K_{pu} values and the log of Eq. 9 were used to fit a and b, with no additional weighting (log transformation results in 1/Y weighting). Outliers were identified using the BoxWhisker function (Frigge et al., 1989) in Mathematica with outliers defined as > 1.5 times the interquartile range. Another model, which included an additional parameter for partitioning into adipose, was evaluated but did not

DMD Fast Forward. Published on July 19, 2019 as DOI: 10.1124/dmd.119.087973
This article has not been copyedited and formatted. The final version may differ from this version.

improve predictions. The lipid concentrations multiplied by the lipid binding constant, L times K_L, (LKL), was calculated from f_{um} with Equation 10, using f_{um} values normalized to 1 mg/mL microsomal protein.

$$LKL = L \times K_L = \frac{1-f_{um}}{f_{um}} \quad \text{Eq. 10}$$

Exposure Overlap Coefficients (EOCs) were used to quantify the ability to predict the shape of the concentration-time profile (Equation 11) (Nagar et al., 2017). They are calculated by determining the overlapping portion of the experimental and predicted C-t profile curves and dividing that area by the experimental area under the curve (AUC). Since the experimental clearance values were used for all predictions, both experimental and predicted C-t profiles will have the same AUC. This allows the EOC to be used as a direct comparison of curve shapes. Differences in the average EOCs were determined using the t-test.

$$EOC = \frac{Overlapping\ Area}{AUC} \quad \text{Eq. 11}$$

V_{ss} Predictions

V_{ss} was determined from the predicted K_p values and physiologic volumes (Equation 12).

$$Vss = Vp + \sum Vt \cdot Kp \quad \text{Eq. 12}$$

where V_p is the plasma volume, and V_t represents the tissue volume.

Predicted V_{ss} values were compared to observed values determined by compartmental modeling. To evaluate the predictive precision of the two methods, the absolute fold-error and average absolute fold error (AAFE) values were determined for all compounds, and for different subsets. Significance of differences in absolute fold errors were determined with a one-tailed T-test. The AAFE determines the geometric mean of the absolute fold error (Equation 13) and is a measure of how precisely the two methods predict V_{ss}.

$$AAFE = 10^{\frac{1}{n}\Sigma|\log FE|} \quad \text{Eq. 13}$$

where n is the number of drugs, and FE is the fold error.

Results

The parameters a and b in Eq. 9 were fit to the experimental tissue reported K_{pu} values for the rat (Rodgers et al., 2005; Rodgers and Rowland, 2006). After sequential removal of twenty outliers (out of 401), optimized parameters were a = 1383 ± 85 and b = 0.096 ± 0.029. The predicted versus observed K_{pu} values for 381 drugs are shown in Figure 2. The R^2 value for the fit was 0.80. There was no consistent characteristic for the removed outliers with the exception of the over-prediction of phencyclidine in four tissues, and the under-prediction of basic compounds in the lung (five drugs).

Figure 3 and Table 3 show the observed versus predicted V_{ss} values using either the $K_{p,dPL}$ prediction method or the $K_{p,mem}$ prediction method. The accuracy of the V_{ss} predictions was analyzed by determining the percent of predictions within a range of absolute fold errors (Table 4) and AAFE (Table 5). For the total dataset of 19 drugs, the $K_{p,mem}$ and $K_{p,dPL}$ methods had comparable AAFE values (2.12 and 2.27, respectively). The $K_{p,mem}$ and $K_{p,dPL}$ methods had one (mibefradil) and two (diphenhydramine, felodipine) outliers, respectively. When these were excluded, the AAFE were again comparable.

Ten different categories were compared in Tables 4 and 5. For predictions less than 1.5 fold error, $K_{p,mem}$ scored higher in 5 categories, lower in 2 categories, and the same in 3 categories as $K_{p,dPL}$ (Table 4). For predictions less than 3 fold error, $K_{p,mem}$ scored lower in 5 categories and the same in 5 categories as $K_{p,dPL}$. When comparing all 19 drugs, the AAFE with $K_{p,mem}$ versus $K_{p,dPL}$ was 2.12 versus 2.27, respectively (Table 5). Across the 10 categories, the AAFE was lower for $K_{p,mem}$ than $K_{p,dPL}$ in 8 categories. When outliers were excluded in each method, the AAFE was lower for $K_{p,mem}$ than $K_{p,dPL}$ in 5 categories. For all categories in Table 5, there were no statistically significant differences in average fold error between $K_{p,mem}$ and $K_{p,dPL}$.

Simulations

An example of EOC calculation is shown in Figure 4 for verapamil. Concentration profiles were simulated for nineteen drugs with both K_p prediction methods (Figures 5 - 7). EOCs were determined for all nineteen drugs (Table 3). Overall, there is no significant difference in the average EOC values for the $K_{p,mem}$ or $K_{p,dPL}$ method. However, there were some interesting deviations between the methods. C-t profiles were poorly predicted by both methods for five drugs:

DMD Fast Forward. Published on July 19, 2019 as DOI: 10.1124/dmd.119.087973
This article has not been copyedited and formatted. The final version may differ from this version.

mibefradil, diazepam, felodipine, diclofenac, and nafcillin. In addition, the $K_{p,dPL}$ method poorly predicted the profiles for betaxolol and diphenhydramine. Some possible explanations for these discrepancies are discussed below.

As discussed previously (Korzekwa and Nagar, 2017b), Eqs. 5-7 indicate that $K_{pu,tissue}$ and ultimately $V_{ss,u}$ should be proportional to $K_{pu,BC}$ (Eq. 7), first experimentally observed by Hinderling (Hinderling, 1997). Also, f_{up} in the denominator of Eq. 7 is ultimately multiplied by f_{up} in the PBPK framework (Eq. 8). Therefore, predicted V_{ss} values for bases should be relatively insensitive to f_{up} when using Eqs. 4-7. The impact on predicted V_{ss} after a 2-fold decrease in f_{up} is shown in Table 6. As expected, changing f_{up} for acids has little effect, since plasma protein binding is high and V_{ss} is low. For neutrals, a 2-fold decrease in f_{up} results in an average 1.7-fold increase in V_{ss} for both methods. For bases, a 2-fold decrease in f_{up} results in an average 2-fold decrease in V_{ss} for $K_{p,mem}$, but an average 1.05-fold increase with $K_{p,dPL}$.

DMD Fast Forward. Published on July 19, 2019 as DOI: 10.1124/dmd.119.087973
This article has not been copyedited and formatted. The final version may differ from this version.

Discussion

Tissue partition coefficients, and ultimately V_{ss} are determined primarily by competition between plasma protein binding and lipid partitioning. The $K_{p,dPL}$ method considers binding to neutral lipids such as triglycerides and neutral phospholipids in membranes, with acidic phospholipids considered separately (Rodgers et al., 2005; Rodgers and Rowland, 2006). The method assumes that neutral molecules only interact with neutral phospholipids, and only ionized bases interact with acidic phospholipids, an assumption questioned previously (Korzekwa and Nagar, 2017b). The major acidic phospholipid is phosphatidylserine and major neutral phospholipid is phosphatidylcholine. Although phosphatidylcholine is net neutral and phosphatidylserine is net acidic, both molecules are zwitterions. Interactions between charged species in the polar head group region are dynamic processes with conformational changes occurring in a picosecond time-frame (Tieleman et al., 1997). Balaz compiled experimental data evaluating the orientation of exogenous molecules in membranes (Balaz, 2009). Hydrophilic molecules accumulate in the polar headgroup region, amphiphilic molecules at the interface, and hydrophobic molecules in the hydrophobic core. We have used this concept to develop quantitative models for membrane partitioning (Nagar and Korzekwa, 2017).

The $K_{p,mem}$ model is based on previously reported V_{ss} models (Korzekwa and Nagar, 2017a). The K_p model described here uses the phospholipid component of tissues and f_{um} to model membrane partitioning, and LogP for neutral lipid interactions. Equation 9 was parameterized using reported tissue composition data and tissue K_p values (Rodgers et al., 2005; Rodgers and Rowland, 2006) . Only two constants were parameterized: *a,* the scaling factor for membranes, and *b* for neutral lipids. Although the two methods use different mechanistic assumptions, the resulting fit for $K_{p,mem}$ (Fig. 2) is similar to that reported by Rodgers for K_{pu} parameterization (Rodgers et al., 2005).

The volume of distribution is generally low for acids due to high plasma protein binding and low partitioning into membranes and neutral lipids. At physiologic pH, most acids are negatively charged, and membranes have few hydrogen bond donors. Therefore, microsomal partitioning is low for acids, with f_{um} values ranging from 0.72-0.98 (Table 2). Both the $K_{p,mem}$ and $K_{p,dPL}$ assume that only the neutral acids partitions into tissues, and both methods predict V_{ss} with similar accuracy (AAFE 2.12 and 2.27 for $K_{p,mem}$ and $K_{p,dPL}$, respectively, Table 5). This is expected since any model that restricts a

DMD Fast Forward. Published on July 19, 2019 as DOI: 10.1124/dmd.119.087973
This article has not been copyedited and formatted. The final version may differ from this version.

compound with low f_{up} to the plasma and extracellular space will predict a V_{ss} approximately equal to that of plasma proteins (~7.5 L)(Rowland and Tozer, 2011). Under-prediction of acids with V_{ss} values > 9, e.g. nafcillin, is frequently observed (Chan et al., 2018). Transporter activity (e.g. OATPs) could be one reason for the under-prediction.

When two outliers for the $K_{p,dPL}$ analysis (diphenhydramine, felodipine) are excluded, V_{ss} predictions for neutrals using $K_{p,dPL}$ improved from an AAFE of 2.82 to 1.91 (Table 5). For diphenhydramine, the $K_{p,dPL}$ method resulted in a 6.9 -fold underprediction and $K_{p,mem}$ gave a 3-fold under-prediction (not an outlier). For felodipine, $K_{p,dPL}$ resulted in a 7.4-fold underprediction and $K_{p,mem}$ gave a 4.3-fold under-prediction (not an outlier). The reason for these poor predictions is unknown but it may be difficult to predict V_{ss} of a highly protein bound and highly partitioned neutral compound (felodipine).

$K_{p,mem}$ uses a single equation for bases, neutrals, and acids and predicts V_{ss} for bases with similar accuracy to $K_{p,dPL}$ which uses different equations for bases (Eqs. 5-7). $K_{p,dPL}$ assumes that ionized bases only interact with acidic phospholipids. This interaction is parameterized with BP, using the erythrocyte partition coefficient to parameterize binding of the ionized base to acidic phospholipids. Mechanistically, the assumption that bases bind only to acidic phospholipids is questionable. Hydrophobic bases bind to neutral phospholipid as well, with key interactions between the cation and negatively charged phosphate, and the hydrophobic region with the hydrophobic membrane core. From Equations 5-7, it is clear that for moderate to strong bases with V_{ss} > total body water, K_p values are dominated by the acidic phospholipid binding terms. Therefore, although binding to only acidic phospholipids was assumed, a similar relationship is possible, assuming that ionized bases bind to all phospholipids. The ratio of neutral to acidic phospholipids is relatively constant across tissues (CV = 15%)(Rodgers et al., 2005), and total phospholipids can be substituted for neutral phospholipids. The K_{BC} term in Eq 6 would be smaller, but the relevant phospholipid term in Eq. 5 would be larger.

Another implication of using BP to predict K_{pu} for bases is the insensitivity of V_{ss} to measured f_{up}. For acids, V_{ss} is insensitive to f_{up} since tissue partitioning is minimal. V_{ss} values for bases are expected to be proportional to f_{up} since they partition heavily into tissues from the unbound concentration in cytosol (assumed to be equal to the unbound

concentration in plasma). This is observed for $K_{p,mem}$ but not for $K_{p,dPL}$ (Table 6). This is a consequence of using BP (which includes f_{up}) to calculate K_{pu}. V_{ss} predictions can be relatively accurate when BP is used to predict K_p for bases, since errors in f_{up} are not manifest and unbound V_{ss} for bases is proportional to erythrocyte partitioning (Hinderling, 1997). However, errors in f_{up} can still result in many other inaccuracies, including in predictions of clearance and target activity.

Overall, the $K_{p,mem}$ and $K_{p,dPL}$ models give similarly accurate predictions, explaining 68 and 63 percent of the variance in V_{ss} (80 and 79 percent without outliers), respectively. Several factors may explain the remaining variance. First, there can be significant variability in the V_{ss} measured across clinical studies. Not all pharmacokinetic datasets provide body weights. Also, experimental data from multiple sources are used, e.g. BP values. Graham et al. observed a 7% decrease in accuracy when predicted instead of experimental LogP values were used (Graham et al. 2012). For f_{up}, differences between laboratories can be very large. Several recent publications discuss assay conditions for protein binding, including dilution and use of CO_2 (Kochansky et al., 2008; Curran et al., 2011; Di et al., 2017). In this study, we measured an f_{up} of 0.03 for mibefradil, whereas a value of <0.005 was reported previously (Clozel et al.1991). Use of a smaller f_{up} would result in a better prediction with $K_{p,mem}$, but exclusion of our data is not justified.

Lysosomal partitioning affects tissue distribution for bases. For strong bases, partitioning into lysosomes due to pH differences results in lysosomal concentrations >200 times cytosolic concentrations. Assuming 5% lysosomes and 60% intracellular water in cells, partitioning of a strong base into lysosomes can increase the K_{pu} six-fold. As discussed previously, whereas lysosomal partitioning certainly occurs, it is likely to be highly correlated with phospholipid partitioning of bases (Korzekwa and Nagar, 2017a). Finally, although the vegetable oil: water partition constant would be a good surrogate for adiposomes if measured, this value is typically modeled using LogP, which is not necessarily accurate (Korzekwa and Nagar, 2017b).

Transporter-mediated distribution can result in inaccurate predictions of K_p and V_{ss}, particularly for some acids. OATP transporters can alter hepatic intracellular concentrations by two orders of magnitude (Kulkarni et al., 2016). Therefore, uptake into this organ alone can result in a 2-fold increase in V_{ss}. Efflux transporters (e.g. P-gp and BCRP) will have a smaller impact. The decrease in V_{ss} due to P-gp and BCRP at the blood-brain barrier would result in a 2% decrease in Vss.

DMD Fast Forward. Published on July 19, 2019 as DOI: 10.1124/dmd.119.087973
This article has not been copyedited and formatted. The final version may differ from this version.

The impact from the liver would be even smaller since efflux transporters in the apical membrane would only decrease liver concentrations by 50% (Korzekwa and Nagar, 2014).

Since AUC is determined by experimental clearance and dose for both methods, the AUC values for the simulations are normalized, and the EOC captures differences in the shape of the C-t profile (Figure 4). Several C-t profiles in Figures 5-7 are not well-predicted by either method. Although there are differences in the EOC for some drugs, the average EOC for the $K_{p,mem}$ and $K_{p,dPL}$ prediction methods were not significantly different. Since clearance is constant, when V_{ss} is overpredicted (e.g. betaxolol using $K_{p,dPL}$, and mibefradil using $K_{p,mem}$, Fig. 5), the terminal half-life is overpredicted. When V_{ss} is underpredicted (e.g. diphenhydramine using $K_{p,dPL}$, Fig. 5), the terminal half-life is underpredicted. Perhaps the most significant deficiency of the reported modeling approaches is the assumption of perfusion-limited distribution. As seen with diazepam, felodipine, diclofenac and nafcillin, accurate C-t profiles are not predicted even when V_{ss} is well-predicted. For verapamil (Figs. 4 and 5) the distribution phase is not well predicted, presumably due to a combination of using a perfusion-limited model and an experimental clearance. Clearly, multi-compartmental distribution is not accurately modeled with perfusion-limited distribution.

In conclusion, $K_{p,mem}$ can be used to predict K_{pu} with accuracy similar to $K_{p,dPL}$. An advantage of using f_{um} to parameterize membrane partitioning is that f_{um} is used for clearance prediction and is generated early in the discovery/development process. Also, differentiating between acidic and neutral phospholipids for bases and using 0.3 P for neutral compounds is not mechanistically justified. Finally, since both the extent and rate of membrane partitioning and permeability are important, a mechanistically sound basis for membrane interactions is necessary for improved physiologic PK models.

Authorship Contributions:

Participated in research design: Holt, Nagar, and Korzekwa

Conducted experiments: Holt, and Ye

Performed data analysis: Holt, Nagar, and Korzekwa

Wrote or contributed to the writing of the manuscript: Holt, Nagar, and Korzekwa

References

Agarwal SK, Kriel RL, Brundage RC, Ivaturi VD, and Cloyd JC (2013) A pilot study assessing the bioavailability and pharmacokinetics of diazepam after intranasal and intravenous administration in healthy volunteers. *Epilepsy Res* **105:**362-367.

Akaike T (1974) A new look at the statistical model identification. *IEEE Trans Automat Contr* **19:**716-723.

Albert KS, Hallmark MR, Sakmar E, Weidler DJ, and Wagner JG (1975) Pharmacokinetics of diphenhydramine in man. *Journal of Pharmacokinetics and Biopharmaceutics* **3:**159-170.

Arundel P (1997) A multi-compartmental model generally applicable to physiologically-based pharmacokinetics., in: *IFAC Symposium*, University of Warwick, UK.

Austin RP, Barton P, Cockroft SL, Wenlock MC, and Riley RJ (2002) The influence of nonspecific microsomal binding on apparent intrinsic clearance, and its prediction from physicochemical properties. *Drug Metab Dispos* **30:**1497-1503.

Avdeef A (2003) *Absorption and Drug Development: Solubility, Permeability, and Charge State.* Wiley.

Balaz S (2009) Modeling Kinetics of Subcellular Disposition of Chemicals. *Chem Rev* **109:**1793-1899.

Berezhkovskiy LM (2004) Volume of distribution at steady state for a linear pharmacokinetic system with peripheral elimination. *J Pharm Sci* **93:**1628-1640.

Björkman S (2002) Prediction of the volume of distribution of a drug: Which tissue-plasma partition coefficients are needed? *J Pharm Pharmacol* **54:**1237-1245.

Blanchard J and Sawers SJA (1983) The absolute bioavailability of caffeine in man. *Eur J Clin Pharmacol* **24:**93-98.

Brittain He (2007.) *Profiles of Drug Substances, excipients, and related methodology*. Academic Press.

Brown RP, Delp MD, Lindstedt SL, Rhomberg LR, and Beliles RP (1997) Physiological parameter values for physiologically based pharmacokinetic models. *Toxicol Ind Health* **13:**407-484.

Campbell BC, Kelman AW, and Hillis WS (1985) Noninvasive assessment of the hemodynamic-effects of Nicardipine in normotensive subjects. *Br J Clin Pharmacol* **20:**S55-S61.

Chan R, De Bruyn T, Wright M, and Broccatelli F (2018) Comparing Mechanistic and Preclinical Predictions of Volume of Distribution on a Large Set of Drugs. *Pharm Res* **35:**11.

Clozel JP, Osterrieder W, Kleinbloesem CH, Welker HA, Schlappi B, Tudor R, Hefti F, Schmitt R, and Eggers H (1991) RO 40-5967 - A new nonhydropyridine calcium-antagonist. *Cardiovasc Drug Rev* **9:**4-17.

Curran RE, Claxton CRJ, Hutchison L, Harradine PJ, Martin IJ, and Littlewood P (2011) Control and Measurement of Plasma pH in Equilibrium Dialysis: Influence on Drug Plasma Protein Binding. *Drug Metab Dispos* **39:**551.

De Buck SS, Sinha VK, Fenu LA, Gilissen RA, Mackie CE, and Nijsen MJ (2007) The prediction of drug metabolism, tissue distribution, and bioavailability of 50 structurally diverse compounds in rat using mechanism-based absorption, distribution, and metabolism prediction tools. *Drug Metab Dispos* **35:**649-659.

Debruyne D (1997) Clinical pharmacokinetics ol fluconazole in superficial and systemic mycoses. *Clin Pharmacokinet* **33:**52-77.

Debruyne D, Hurault de Ligny B, P Ryckelynck J, Albessard F, and Moulin M (1987) *Clinical Pharmacokinetics of Ketoprofen After Single Intravenous Administration as a Bolus or Infusion*.

Di L, Breen C, Chambers R, Eckley ST, Fricke R, Ghosh A, Harradine P, Kalvass JC, Ho S, Lee CA, Marathe P, Perkins EJ, Qian M, Tse S, Yan ZY, and Zamek-Gliszczynski MJ (2017) Industry Perspective on Contemporary Protein-Binding Methodologies: Considerations for Regulatory Drug-Drug Interaction and Related Guidelines on Highly Bound Drugs. *J Pharm Sci* **106:**3442-3452.

Diez I, Colom H, Moreno J, Obach R, Peraire C, and Domenech J (1991) A Comparative in-vitro study of transdermal absorption of a series of calcium-channel antagonists. *J Pharm Sci* **80:**931-934.

Edgar B, Regardh CG, Johnsson G, Johansson L, Lundborg P, Lofberg I, and Ronn O (1985) Felodipine Kinetics in Healthy-Men. *Clin Pharmacol Ther* **38:**205-211.

Fenneteau F, Poulin P, and Nekka F (2010) Physiologically Based Predictions of the Impact of Inhibition of intestinal and Hepatic Metabolism on Human Pharmacokinetics of CYP3A Substrates. *J Pharm Sci* **99:**486-514.

Frigge M, Hoaglin DC, and Iglewicz B (1989) Some Implementations of the Boxplot. **43:**50.

Ghafourian T, Barzegar-Jalali M, Hakimiha N, and Cronin MTD (2004) Quantitative structure-pharmacokinetic relationship modelling: apparent volume of distribution. *J Pharm Pharmacol* **56:**339-350.

Graham H, Walker M, Jones O, Yates J, Galetin A, and Aarons L (2012) Comparison of in-vivo and in-silico methods used for prediction of tissue: plasma partition coefficients in rat. *J Pharm Pharmacol* **64:**383-396.

Greene DS, Quintiliani R, and Nightingale CH (1978) Physiological perfusion model for cephalosporin antibiotics I: Model selection based on blood drug concentrations. *J Pharm Sci* **67:**191-196.

Gugler R, Manion CV, and Azarnoff DL (1976) Phenytoin- Pharmacokinetics and Bioavailability. *Clin Pharmacol Ther* **19:**135-142.

Hallifax D and Houston JB (2006) Binding of drugs to hepatic microsomes: Comment and assessment of current prediction methodology with recommendation for improvement. *Drug Metab Dispos* **34:**724-726.

Hansch C, A. L, and DH. H (1995) Exploring QSAR: Hydrophobic, Electronic, and Steric Constraints, ACS Publications

Heizmann P, Eckert M, and Ziegler WH (1983) Pharmacokinetics and Bioavailability of Midazolam in Man. *Br J Clin Pharmacol* **16:**S43-S49.

Hermann P, Rodger SD, Remones G, Thenot JP, London DR, and Morselli PL (1983) Pharmacokinetics of Diltiazem After Intravenous and Oral-Administration. *Eur J Clin Pharmacol* **24:**349-352.

Hinderling PH (1997) Red blood cells: a neglected compartment in pharmacokinetics and pharmacodynamics. *Pharmacol Rev* **49:**279-295.

Hiskey CF, Whitman G, and Bullock E (1962) Spectrophotometric Study of Aqueous Solution of Warfarin Sodium. *J Pharm Sci* **51:**43-&.

Ishihama Y, Nakamura M, Miwa T, Kajima T, and Asakawa N (2002) A rapid method for pK(a) determination of drugs using pressure-assisted capillary electrophoresis with photodiode array detection in drug discovery. *J Pharm Sci* **91:**933-942.

Jansson R, Bredberg U, and Ashton M (2008) Prediction of drug tissue to plasma concentration ratios using a measured volume of distribution in combination with lipophilicity. *J Pharm Sci* **97:**2324-2339.

Jones R, Jones HM, Rowland M, Gibson CR, Yates JWT, Chien JY, Ring BJ, Adkison KK, Ku MS, He HD, Vuppugalla R, Marathe P, Fischer V, Dutta S, Sinha VK, Bjornsson T, Lave T, and Poulin P (2011) PhRMA CPCDC Initiative on Predictive Models of Human Pharmacokinetics, Part 2: Comparative Assessment of Prediction Methods of Human Volume of Distribution. *J Pharm Sci* **100:**4074-4089.

Kochansky CJ, McMasters DR, Lu P, Koeplinger KA, Kerr HH, Shou M, and Korzekwa KR (2008) Impact of pH on plasma protein binding in equilibrium dialysis. *Mol Pharm* **5:**438-448.

Korzekwa K and Nagar S (2014) Compartmental Models for Apical Efflux by P-glycoprotein: Part 2-A Theoretical Study on Transporter Kinetic Parameters. *Pharm Res* **31:**335-346.

Korzekwa K and Nagar S (2017a) Drug Distribution Part 2. Predicting Volume of Distribution from Plasma Protein Binding and Membrane Partitioning. *Pharm Res* **34:**544-551.

Korzekwa K and Nagar S (2017b) On the Nature of Physiologically-Based Pharmacokinetic Models -A Priori or A Posteriori? Mechanistic or Empirical? *Pharm Res* **34:**529-534.

Kulkarni P, Korzekwa K, and Nagar S (2016) Intracellular Unbound Atorvastatin Concentrations in the Presence of Metabolism and Transport. *J Pharmacol Exp Ther* **359:**26-36.

Leo A, Hansch C, and Elkins D (1971) Partition coefficients and their uses. *Chem Rev* **71:**525-616.

Li R, Bi YA, Vildhede A, Scialis RJ, Mathialagan S, Yang X, Marroquin LD, Lin J, and Varma MVS (2017) Transporter-Mediated Disposition, Clinical Pharmacokinetics and Cholestatic Potential of Glyburide and Its Primary Active Metabolites. *Drug Metab Dispos* **45:**737-747.

Lombardo F, Obach RS, DiCapua FM, Bakken GA, Lu J, Potter DM, Gao F, Miller MD, and Zhang Y (2006) Hybrid mixture discriminant analysis-random forest computational model for the prediction of volume of distribution of drugs in human. *J Med Chem* **49:**2262-2267.

Lombardo F, Obach RS, Shalaeva MY, and Gao F (2004) Prediction of human volume of distribution values for neutral and basic drugs. 2. Extended data set and leave-class-out statistics. *J Med Chem* **47:**1242-1250.

Ludden TM, Boyle DA, Gieseker D, Kennedy GT, Crawford MH, Ludden LK, and Clementi WA (1988) Absolute Bioavailability and Dose Proportionality of Betaxolol in Normal Healthy-Subjects. *J Pharm Sci* **77:**779-783.

Maguire KP, Burrows GD, Norman TR, and Scoggins BA (1980) Blood-Plasma Distribution Ratios of Psychotropic-Drugs. *Clin Chem* **26:**1624-1625.

McAllister RG and Kirsten EB (1982) The Pharmacology of Verapmail. IV. Kinetics and Dynamic Effects After Single Intravenous and Oral Doses. *Clin Pharmacol Ther* **31:**418-426.

Nagar S and Korzekwa K (2012) Commentary: Nonspecific Protein Binding versus Membrane Partitioning: It Is Not Just Semantics. *Drug Metab Dispos* **40:**1649-1652.

Nagar S and Korzekwa K (2017) Drug Distribution. Part 1. Models to Predict Membrane Partitioning. *Pharm Res* **34:**535-543.

Nagar S, Korzekwa RC, and Korzekwa K (2017) Continuous Intestinal Absorption Model Based on the Convection-Diffusion Equation. *Mol Pharm* **14:**3069-3086.

Nagar S, Tucker J, Weiskircher EA, Bhoopathy S, Hidalgo IJ, and Korzekwa K (2014) Compartmental Models for Apical Efflux by P-glycoprotein-Part 1: Evaluation of Model Complexity. *Pharm Res* **31:**347-359.

O'Neil M (2006) *The Merck Index- An Encyclopedia of Chemicals, Drugs, and Biologicals*. Merck and Co, Inc., Whitehouse Station, NJ.

O'Reilly RA, Welling PG, and Wagner JG (1971) Pharmacokinetics of Warfarin following intravenous administration to man. *Thrombosis Et Diathesis Haemorrhagica* **25:**178-&.

Obach RS (1999) Prediction of human clearance of twenty-nine drugs from hepatic microsomal intrinsic clearance data: An examination of in vitro half-life approach and nonspecific binding to microsomes. *Drug Metab Dispos* **27:**1350-1359.

Obach RS, Baxter JG, Liston TE, Silber BM, Jones BC, MacIntyre F, Rance DJ, and Wastall P (1997) The prediction of human pharmacokinetic parameters from preclinical and in vitro metabolism data. *J Pharmacol Exp Ther* **283:**46-58.

Oie S and Tozer TN (1979) Effect of Altered Plasma-Protein Binding on Apparent Volume of Distribution. *J Pharm Sci* **68:**1203-1205.

Pandey M, Arikotla J, Kumar A, Malik R, and Charde SY (2013) *Determination of pKa of felodipine using UV–Visible spectroscopy*.

Poulin P and Haddad S (2011) Microsome Composition-Based Model as a Mechanistic Tool to Predict Nonspecific Binding of Drugs in Liver Microsomes. *J Pharm Sci* **100:**4501-4517.

Poulin P and Krishnan K (1995) A biologically-based algorithm for predicting human tissue-blood partition coefficients of organic chemicals. *Hum Exp Toxicol* **14:**273-280.

Poulin P, Schoenlein K, and Theil FP (2001) Prediction of adipose tissue : plasma partition coefficients for structurally unrelated drugs. *J Pharm Sci* **90:**436-447.

Poulin P and Theil FP (2000) A Priori prediction of tissue : plasma partition coefficients of drugs to facilitate the use of physiologically-based pharmacokinetic models in drug discovery. *J Pharm Sci* **89:**16-35.

Poulin P and Theil FP (2002) Prediction of pharmacokinetics prior to in vivo studies. 1. Mechanism-based prediction of volume of distribution. *J Pharm Sci* **91:**129-156.

Poulin P and Theil FP (2009) Development of a Novel Method for Predicting Human Volume of Distribution at Steady-State of Basic Drugs and Comparative Assessment With Existing Methods. *J Pharm Sci* **98:**4941-4961.

Recanatini M (1992) Partition and Distribution Coefficients of Aryloxypropanolamine Beta-Adrenoceptor Antagonists. *J Pharm Pharmacol* **44:**68-70.

Regårdh C, Borg K, Johansson R, Johnsson G, and Palmer L (1974) Pharmacokinetic studies on the selective beta1-receptor antagonist metoprolol in man. *Journal of Pharmacokinetics and Biopharmaceutics* **2:**347-364.

Rekker R and Mannhold R (1992) *Calculation of drug lipophilicity: the hydrophobic fragmental constant approach*. VCH.

Riddell JG, Harron DWG, and Shanks RG (1987) Clinical pharmacokinetics of beta-adrenoceptor antagonists- An Update. *Clin Pharmacokinet* **12:**305-320.

Ripa S, Ferrante L, and Prenna M (1993) Pharmacokinetics of Fluconazole in Normal Volunteers. *Chemotherapy* **39:**6-12.

Robinson MA and Mehvar R (1996) Enantioselective distribution of verapamil and norverapamil into human and rat erythrocytes: The role of plasma protein binding. *Biopharm Drug Dispos* **17:**577-587.

Rodgers T, Leahy D, and Rowland M (2005) Physiologically based pharmacokinetic modeling 1: Predicting the tissue distribution of moderate-to-strong bases. *J Pharm Sci* **94:**1259-1276.

Rodgers T and Rowland M (2006) Physiologically based pharmacokinetic modelling 2: Predicting the tissue distribution of acids, very weak bases, neutrals and zwitterions. *J Pharm Sci* **95:**1238-1257.

Rodgers T and Rowland M (2007) Mechanistic approaches to volume of distribution predictions: Understanding the processes. *Pharm Res* **24:**918-933.

Rowland M and Tozer TN (2011) Distribution of Drugs Extensively Bound to Plasma Proteins, in: *Clinical Pharmacokinetics and Pharmacodynamics: Concepts And Applications*, pp 695-701, Wolters Kluwer Health/Lippincott William & Wilkins, Philadelphia, PA.

Sangster J (1993) LOGKOW- a DataBank of evaluated octanol-water partition coefficients. (Laboratories SR ed, Montreal.

Sangster J (1994) *Octanol-Water Partition-Coefficients: Fundamentals and Physical Chemistry.* Wiley, New York.

Scavone JM, Luna BG, Harmatz JS, Von Moltke L, and Greenblatt DJ (1990) Diphenhydramine kinetics following intravenous, oral, and sublingual dimenhydrinate administration. **11:**185-189.

Stella VJ, Martodihardjo S, Terada K, and M. Rao V (1998) Some relationships between the physical properties of various 3-acyloxymethyl prodrugs of phenytoin to structure: Potential in vivo performance implications. *J Pharm Sci* **87:**1235-1241.

Tieleman DP, Marrink SJ, and Berendsen HJC (1997) A computer perspective of membranes: molecular dynamics studies of lipid bilayer systems. *Biochimica et Biophysica Acta (BBA) - Reviews on Biomembranes* **1331:**235-270.

Uchimura T, Kato M, Saito T, and Kinoshita H (2010) Prediction of Human Blood-to-Plasma Drug Concentration Ratio. *Biopharm Drug Dispos* **31:**286-297.

Ueda CT, Hirschfeld DS, Scheinman MM, Rowland M, Williamson BJ, and Dzindzio BS (1976) Disposition Kinetics of Quinidine. *Clin Pharmacol Ther* **19:**30-36.

Waller ES, Sharanevych MA, and Yakatan GJ (1982) The Effect of Probenecid on Nafcillin Disposition. *J Clin Pharmacol* **22:**482-489.

Welker HA, Wiltshire H, and Bullingham R (1998) Clinical pharmacokinetics of mibefradil. *Clin Pharmacokinet* **35:**405-423.

Willis JV, Kendall MJ, and Jack DB (1980) A Study of the Effect of Aspirin on the Pharmacokinetics of Oral and Intravenous Diclofenac Sodium. *Eur J Clin Pharmacol* **18:**415-418.

Wishart DS, Feunang YD, Guo AC, Lo EJ, Marcu A, Grant JR, Sajed T, Johnson D, Li C, Sayeeda Z, Assempour N, Iynkkaran I, Liu YF, Maciejewski A, Gale N, Wilson A, Chin L, Cummings R, Le D, Pon A, Knox C, and Wilson M (2018) DrugBank 5.0: a major update to the DrugBank database for 2018. *Nucleic Acids Res* **46:**D1074-D1082.

Ye M, Nagar S, and Korzekwa K (2016) A physiologically based pharmacokinetic model to predict the pharmacokinetics of highly protein-bound drugs and the impact of errors in plasma protein binding. *Biopharm Drug Dispos* **37:**123-141.

Zhivkova Z and Doytchinova I (2012) Prediction of steady-state volume of distribution of acidic drugs by quantitative structure-pharmacokinetics relationships. *J Pharm Sci* **101:**1253-1266.

Zou P, Zheng N, Yang YS, Yu LX, and Sun DX (2012) Prediction of volume of distribution at steady state in humans: comparison of different approaches. *Expert Opin Drug Metab Toxicol* **8:**855-872.

Footnotes

This research was supported by National Institutes of Health grants [R01GM104178 and R01GM114369].

DMD Fast Forward. Published on July 19, 2019 as DOI: 10.1124/dmd.119.087973
This article has not been copyedited and formatted. The final version may differ from this version.

Figure Legends

Figure 1. Scheme for the generic PBPK model used in this study.

Figure 2. Observed versus predicted rat K_{pu} values from Eq. 10. blue - adipose, red - bone, green - brain, purple - gut, lt. blue - heart, orange - kidney, magenta - liver, yellow - lung, lt. green - muscle, brown - skin, black – spleen.

Figure 3. Observed steady-state volume of distribution (V_{ss}) vs predicted V_{ss} for 19 drugs. Blue – $K_{p,dPL}$, red – $K_{p,mem}$.

Figure 4. Determination of the exposure overlap coefficients for verapamil. Red line - simulated concentration-time profile using $K_{p,mem}$ method; blue line - simulated concentration-time profile using $K_{p,dPl}$ method; green area - area of overlap.

Figure 5. Observed and predicted C-t profiles for bases. Red line - simulated concentration-time profile using $K_{p,mem}$ method; blue line - simulated concentration-time profile using $K_{p,dPl}$ method; points – experimental data.

Figure 6. Observed and predicted C-t profiles for neutral molecules. Red line - simulated concentration-time profile using $K_{p,mem}$ method; blue line - simulated concentration-time profile using $K_{p,dPl}$ method; points – experimental data.

Figure 7. Observed and predicted C-t profiles for acids. Red line - simulated concentration-time profile using $K_{p,mem}$ method; blue line - simulated concentration-time profile using $K_{p,dPl}$ method; points – experimental data.

DMD Fast Forward. Published on July 19, 2019 as DOI: 10.1124/dmd.119.087973
This article has not been copyedited and formatted. The final version may differ from this version.

Table 1: Pharmacokinetic Parameters of test drugs.

Name	Class[a]	Type	subjects	Wt	Dose	duration	Points	Vss	CL	Reference
				kg	mg	minutes	#	L	L/h	
Betaxolol	B	infusion	n=10	73.6	8.94	30	17	360	11	(Ludden et al., 1988)
Diltiazem	B	infusion	n=12	63	15	30	13	306	97	(Hermann et al., 1983)
Diphenhydramine	B	bolus	n=8	98.0	56	n/a	12	788	43	(Scavone et al., 1990)
Metoprolol	B	infusion	n=5	66	3.9	10	20	274	59	(Regårdh et al., 1974)
Mibefradil	B	Infusion	n=6	70[c]	20	30	16	187	17	(Clozel et al., 1991)
Nicardipine	B	bolus	n=6[b]	67.0	10	n/a	12	62	76	(Campbell et al., 1985)
Quinidine	B	infusion	n=12[b]	65.3	244	22	12	227	18.5	(Ueda et al., 1976)
Verapamil	B	infusion	n=20	70[c]	10	5	15	266	49	(McAllister and Kirsten, 1982
Caffeine	N	infusion	n=10	79.5	350	30	17	42.8	5.2	(Blanchard and Sawers, 1983
Diazepam	N	infusion	n=24	78.1	5	1	21	89.5	1.33	(Agarwal et al., 2013)
Felodipine	N	infusion	n=10	74	2.5	30	22	320	41.7	(Edgar et al., 1985)
Fluconazole	N	infusion	n=6	70[c]	50	n/a	13	59.3	1.25	(Ripa et al., 1993)
Midazolam	N	bolus	n=6	67.6	10	n/a	15	51.2	18	(Heizmann et al., 1983)
Phenytoin	N	infusion	n=6	78.1	275	6	15	38.8	1.76	(Gugler et al., 1976)
Diclofenac	A	infusion	n=6	65	46.5	2	15	9.23	17.6	(Willis et al., 1980)
Glyburide	A	infusion	n=10	77.8	2	60	19	11.78	4.88	(Debruyne et al., 1987)
Ketoprofen	A	bolus	n=7	70[c]	100	n/a	12	9.9	5.02	(Debruyne et al., 1987)
Nafcillin	A	infusion	n=6	70[c]	475	7	9	20.4	33.9	(Waller et al., 1982)
Warfarin	A	bolus	n=6	66.8	100	n/a	8	7.66	.179	(O'Reilly et al., 1971)

[a] Bases - B, Acids - A, Neutral – N; [b] Individual C-t not provided. C-t profile simulated from average parameters. [c] Individual weights not provided and 70 kg assumed.

DMD Fast Forward. Published on July 19, 2019 as DOI: 10.1124/dmd.119.087973
This article has not been copyedited and formatted. The final version may differ from this version.

Table 2: Drug Specific Parameters.

Compound	Class[a]	f_{up} (n=4)[b]	f_{um} (n=4)[b]	LogP	Pk_{aa}	Pk_{ab}	BP	$LogD_{vo}$	CL (L/h)	References
Betaxolol	B	0.50 (12%)	0.77 (3%)	2.81	14	9.4	2[c]	1.78	10.2	(Riddell et al., 1987; Recanatini, 1992; Rodgers and Rowland, 2007)
Diltiazem	B	0.26 (8%)	0.48 (2%)	2.7	14	7.7	1	1.88	97.5	(Rekker and Mannhold, 1992; Obach, 1999; Ishihama et al., 2002)
Diphenhydramine	B	0.44 (4%)	0.84 (4%)	3.27	14	8.98	0.74	2.30	43	(Albert et al., 1975; Sangster, 1994; Hansch et al., 1995; Obach, 1999)
Metoprolol	B	0.87 (17%)	0.80 (3%)	1.88	14	9.7	1.14	0.746	58.8	(Hansch et al., 1995; Rodgers and Rowland, 2007)
Mibefradil	B	0.031 (11%)	0.034 (15%)	3.07	14	10.2	0.64	2.07	15.5	(Welker et al., 1998; Nagar and Korzekwa, 2017)
Nicardipine	B	0.0024 (7%)	0.039 (12%)	3.82	14	8.6	0.71	2.90	31.2	(Sangster, 1993; Rodgers and Rowland, 2007)
Quinidine	B	0.15 (8%)	0.815 (10%)	3.52	14	8.94	0.92	2.07	14	(Sangster, 1994; Obach, 1999; Nagar and Korzekwa, 2017)
Verapamil	B	0.088 (20%)	0.37 (19%)	3.79	14	8.92	0.74	2.88	49	(Sangster, 1994; Hansch et al., 1995; Robinson and Mehvar, 1996; Obach, 1999)
Caffeine	N	0.72[d]	0.98 (6%)	-0.07	14	1.04	1.01	-1.43	5.2	(Hansch et al., 1995; Rodgers and Rowland, 2007)
Diazepam	N	0.012 (9%)	0.74 (4%)	2.82	14	3.4	0.64	1.79	1.33	(Maguire et al., 1980; Sangster, 1993; O'Neil, 2006)
Felodipine	N	0.0017 (12%)	0.023 (27%)	3.86	14	5.07	0.7	2.95	41.7	(Diez et al., 1991; Uchimura et al., 2010; Pandey et al., 2013)
Fluconazole	N	0.93 (14%)	0.94 (14%)	0.8	14	1.77	1	-0.79	1.25	(Debruyne et al., 1987; Debruyne, 1997; Rodgers and Rowland, 2007)
Midazolam	N	0.033 (4%)	0.71 (4%)	3.15	14	6.01	0.53	2.16	18	(Heizmann et al., 1983; Rodgers and Rowland, 2007)
Phenytoin	N	0.18 (7%)	0.83 (3%)	2.21	8.32	1	0.61	1.11	1.61	(Stella et al., 1998; Brittain, 2007.; Uchimura et al., 2010)
Diclofenac	A	0.0014 (18%)	0.78 (4%)	4.51	4.15	1	0.55	3.68	17.6	(Sangster, 1994; Obach, 1999; Avdeef, 2003)
Glyburide	A	0.0012 (16%)	0.72 (9%)	4.29	5.38	1	0.57	2.59	4.81	(Austin et al., 2002; Li et al., 2017)
Ketoprofen	A	0.0041 (9%)	0.95 (4%)	3.12	4.45	1	0.56	2.06	5.02	(Sangster, 1993; Sangster, 1994; Rodgers and Rowland, 2007; Ye et al., 2016)
Nafcillin	A	0.123 (6%)	0.94 (14%)	2.7	2.6	1	0.55[e]	1.66	33.9	(Wishart et al., 2018)
Warfarin	A	0.0076 (13%)	0.98 (16%)	2.7	5.05	1	0.55	1.66	0.179	(Hiskey et al., 1962; Hansch et al., 1995; Obach, 1999)

[a] Bases - B, Acids - A, Neutral - N. [b]All 98experimental values unless otherwise noted. [c] Rat BP was used. [d] An average of literature values was used. [e]0.55 was used (1-hematocrit).

DMD Fast Forward. Published on July 19, 2019 as DOI: 10.1124/dmd.119.087973
This article has not been copyedited and formatted. The final version may differ from this version.

Table 3: Observed and Predicted V_{ss} and EOC values for both methods.

	Observed V_{ss} (L)	Predicted V_{ss} $K_{p,mem}$ method (L)	Predicted V_{ss} $K_{p,dPL}$ method (L)	EOC $K_{p,mem}$ method	EOC $K_{p,dPL}$ method
Betaxolol	360	307	856	0.97	0.61
Diltiazem	306	320	309	0.76	0.80
Diphenhydramine	788	260	115	0.97	0.87
Metoprolol	274	429	217	0.76	0.87
Mibefradil	187	1470	53.2	0.81	0.82
Nicardipine	62	96.4	98.5	0.79	0.78
Quinidine	227	78.3	215	0.96	0.73
Verapamil	266	258	136	0.73	0.76
Caffeine	42.8	47.0	36.7	0.87	0.93
Diazepam	89.5	22.9	30.5	0.55	0.61
Felodipine	320	74.3	43.4	0.68	0.56
Fluconazole	59.3	83.4	49.1	0.85	0.99
Midazolam	51.2	64.1	113	0.82	0.71
Phenytoin	38.8	77.0	79.1	0.78	0.77
Diclofenac	9.23	7.98	7.89	0.84	0.84
Glyburide	11.78	10.2	10.0	0.86	0.87
Ketoprofen	9.9	8.54	8.47	0.89	0.89
Nafcillin	20.4	12.2	10.1	0.86	0.81
Warfarin	7.66	8.20	8.15	0.96	0.97
			Average	0.82 +/- 0.11	0.80 +/- 0.12

DMD Fast Forward. Published on July 19, 2019 as DOI: 10.1124/dmd.119.087973
This article has not been copyedited and formatted. The final version may differ from this version.

Table 4. Fraction of drugs whose predictions were less than 1.5-, 2-, and 3-fold error.						
	< 1.5-fold error		< 2-fold error		< 3-fold error	
	$K_{p,mem}$	$K_{p,dPL}$	$K_{p,mem}$	$K_{p,dPL}$	$K_{p,mem}$	$K_{p,dPL}$
All Compounds	10/19	9/19	14/19	11/19	15/19	16/19
Acids	4/5	4/5	5/5	4/5	5/5	5/5
Bases	3/8	3/8	5/8	5/8	6/8	6/8
Neutrals	3/6	2/6	4/6	2/6	4/6	5/6
LogP<3	5/9	5/9	8/9	5/9	8/9	9/9
LogP >3	5/10	4/10	6/10	6/10	7/10	7/10
f_{um} < 0.8	6/11	4/11	8/11	6/11	8/11	9/11
f_{um}> 0.8	4/8	5/8	6/8	5/8	7/8	7/8
f_{up} <0.1	6/10	4/10	7/10	6/10	7/10	8/10
f_{up} >0.1	4/9	5/9	7/9	8/9	8/9	8/9

DMD Fast Forward. Published on July 19, 2019 as DOI: 10.1124/dmd.119.087973
This article has not been copyedited and formatted. The final version may differ from this version.

Table 5: Absolute Average Fold Error for V_{ss} predictions using both $K_{p,mem}$ and $K_{p,dPL}$ prediction methods.

	AAFE		AAFE (excluding outliers)	
Category	$K_{p,mem}$	$K_{p,dPL}$	$K_{p,mem}$	$K_{p,dPL}$
All Compounds	2.12	2.27	1.80	1.70
Acids	1.24	1.32	1.24	1.32
Bases	2.52	2.45	1.76	1.82
Neutrals	2.32	2.82	2.32	1.91
LogP<3	1.66	1.68	1.66	1.68
LogP >3	2.54	2.81	1.95	1.73
f_{um} < 80%	2.36	2.41	1.81	1.92
f_{um}> 80%	1.79	2.07	1.79	1.39
f_{up} <10%	2.45	2.42	1.84	1.86
f_{up} >10%	1.76	2.11	1.76	1.56

DMD Fast Forward. Published on July 19, 2019 as DOI: 10.1124/dmd.119.087973
This article has not been copyedited and formatted. The final version may differ from this version.

Table 6. Impact of errors in f_{up} on V_{ss}				
	Fold decrease in V_{ss} upon a 2-fold decrease in f_{up}			
Compound	$K_{p,mem}$		$K_{p,dPL}$	
Betaxolol	1.97		0.95	
Diltiazem	1.98		1.05	
Diphenhydramine	1.94		0.82	
Metoprolol	1.98		0.75	
Mibefradil	2.00		0.95	
Nicardipine	1.90		1.01	
Quinidine	1.89	average (bases)	1.00	average (bases)
Verapamil	1.95	1.95 ± 0.04	1.06	0.95 ± 0.11
Caffeine	1.66		1.59	
Diazepam	1.41		1.53	
Felodipine	1.79		1.66	
Fluconazole	1.82		1.70	
Midazolam	1.78	average (neutrals)	1.86	average (neutrals)
Phenytoin	1.78	1.71 ± 0.15	1.79	1.69 ± 0.12
Diclofenac	1.01		1.01	
Glyburide	1.05		1.03	
Ketoprofen	1.01		1.00	
Nafcillin	1.19	average (acids)	1.09	average (acids)
Warfarin	1.01	1.05 ± 0.08	1.01	1.03 ± 0.04

DMD Fast Forward. Published on July 19, 2019 as DOI: 10.1124/dmd.119.087973
This article has not been copyedited and formatted. The final version may differ from this version.

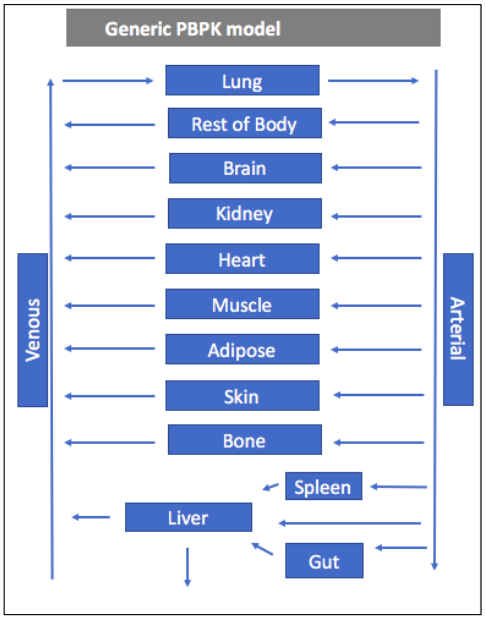

Figure 1.

DMD Fast Forward. Published on July 19, 2019 as DOI: 10.1124/dmd.119.087973
This article has not been copyedited and formatted. The final version may differ from this version.

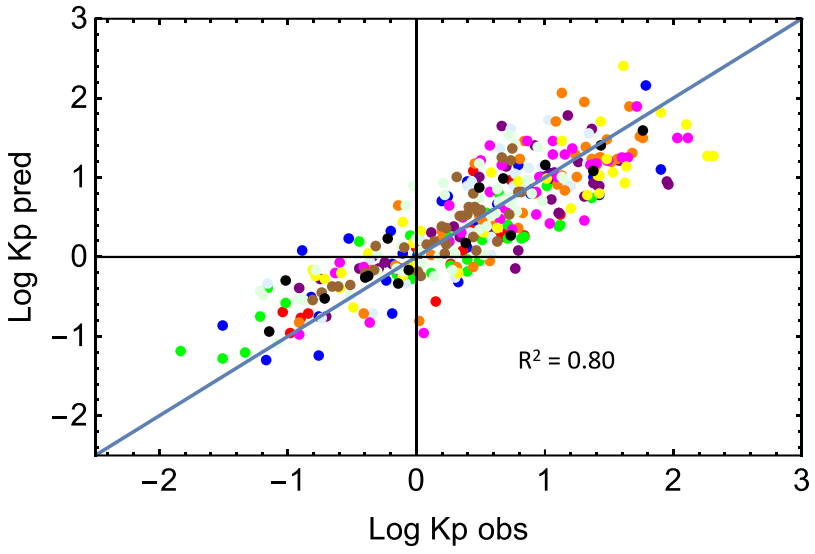

Figure 2.

DMD Fast Forward. Published on July 19, 2019 as DOI: 10.1124/dmd.119.087973
This article has not been copyedited and formatted. The final version may differ from this version.

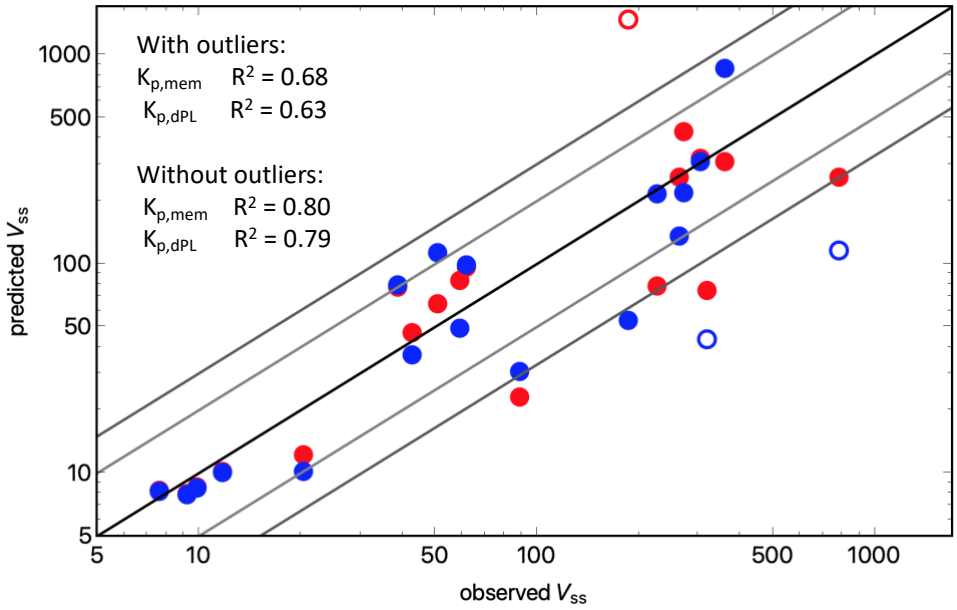

Figure 3.

DMD Fast Forward. Published on July 19, 2019 as DOI: 10.1124/dmd.119.087973
This article has not been copyedited and formatted. The final version may differ from this version.

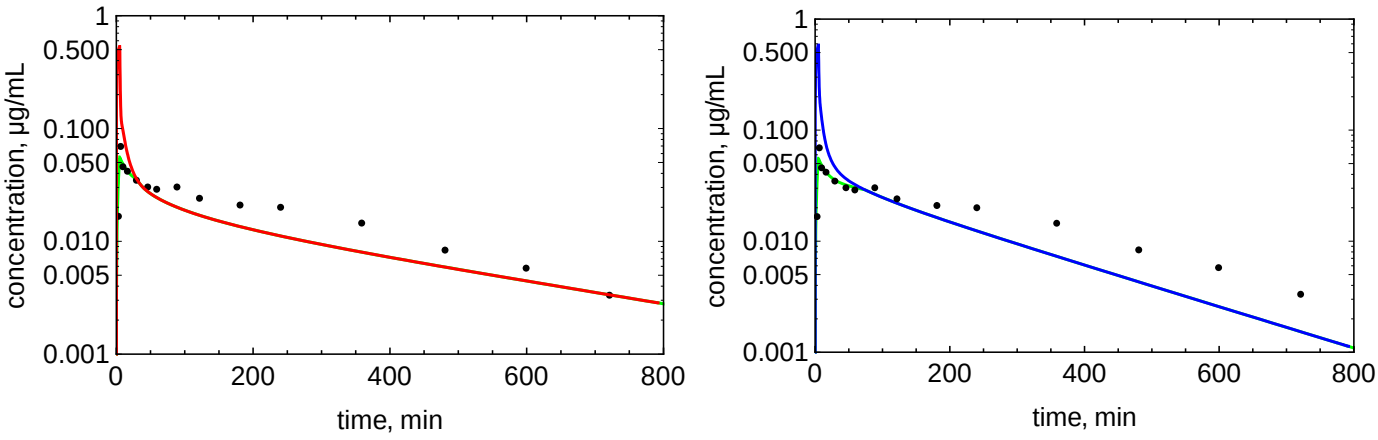

Figure 4.

DMD Fast Forward. Published on July 19, 2019 as DOI: 10.1124/dmd.119.087973
This article has not been copyedited and formatted. The final version may differ from this version.

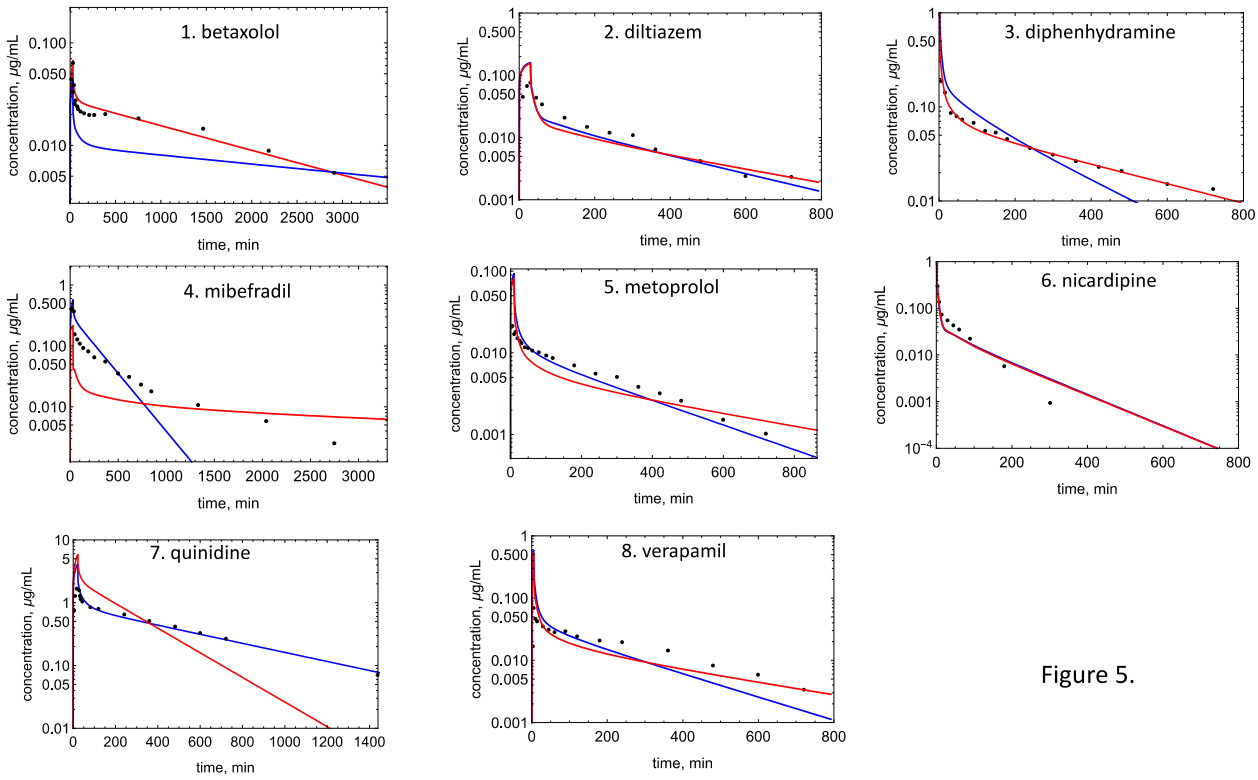

Figure 5.

DMD Fast Forward. Published on July 19, 2019 as DOI: 10.1124/dmd.119.087973
This article has not been copyedited and formatted. The final version may differ from this version.

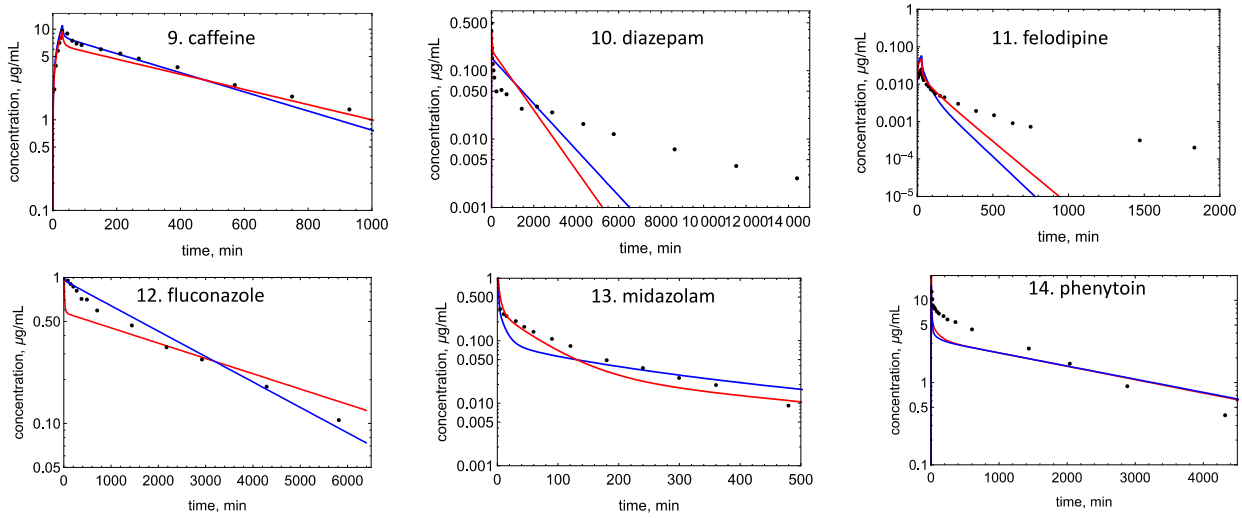

Figure 6.

DMD Fast Forward. Published on July 19, 2019 as DOI: 10.1124/dmd.119.087973
This article has not been copyedited and formatted. The final version may differ from this version.

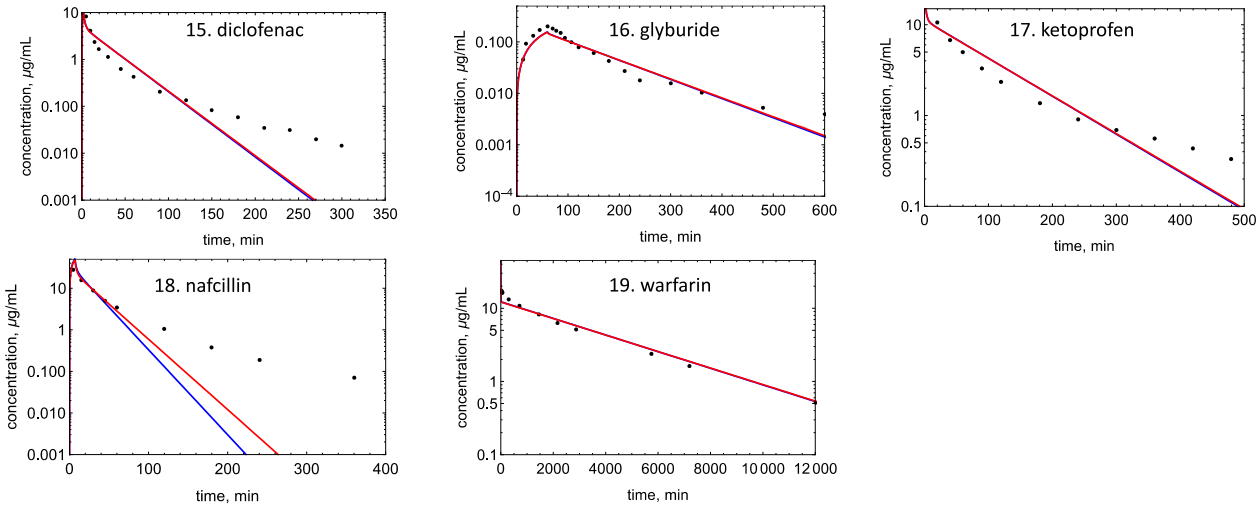

Figure 7.